The formation of 'microlayers' beneath vapour bubbles

Susann Hänsch, Simon Walker

Imperial College London

s.haensch13@imperial.ac.uk

Abstract

'Microlayers', the thin (less than 10 μm) films of liquid left behind beneath rapidly-growing steam bubbles at a heated wall, can be a large, and even the dominant, source of the vapour in such bubbles by the time they depart the wall. Given their slenderness (compared to the 1 to 10 mm diameter of the bubble, and their high aspect ratio, (with radial extents of perhaps order >100 times their thickness), such microlayers are incorporated relatively simplistically in microscopic CFD analyses of bubble growth. However, their role is particularly important because the evaporation of the microlayer generates vapour rapidly, which itself expands the bubble and generates more microlayer and so on. Plainly, a good understanding of the microlayer formation process is desirable. In this paper we present first-principles calculations of the hydrodynamics of the formation of such microlayers. These seem to show that overwhelmingly the determinant of the existence and radial extent of a microlayer is the bubble growth rate, with higher growth rates leading to more flattened and less spherical bubbles, with larger microlayers trapped beneath them. When they *are* formed, microlayer thickness is then to a degree dependent on the fluid surface tension and viscosity. The need for an extension of these hydrodynamic studies to include a mechanistic self-consistent model of the evaporative depletion of the microlayer is noted.

Keywords:

nucleate boiling

microlayer

microlayer thickness

bubble shape

interface-tracking

level-set

1 INTRODUCTION

The boiling process is both intrinsically interesting and industrially important. Component-scale modeling of boiling flows is important in many areas, and particularly so for water-cooled nuclear reactors. Component-scale modeling is necessarily reliant upon semi-empirical representations of the detailed processes of bubble formation, growth and departure, and the associated heat transfers. In recent years microscopic interface-tracking computational fluid dynamics has emerged as a valuable tool to add to the understanding of these processes that could hitherto be gained from only experimental observation.

One of these processes, and the one that is the subject of the present paper, is the formation of 'microlayers'.

At the nucleation site some initial volume of vapour expands at the heated wall, and the vapour-liquid interface thus moves radially upwards and outwards from the nucleation site. Under many circumstances it is observed that a thin layer of liquid water is left behind on the heated surface. This is known as the microlayer. We will discuss dimensions and so on more below, but this layer is typically a few microns thick, and a few hundred microns in radial extent. With its underside at the metal temperature, and its upper surface in contact with essentially saturated vapour, and being very thin, the heat flux through this microlayer can be very large, and consequently its rate of evaporation is also very high. It evaporates quickly, and generates a very rapid increase in the volume of the bubble. The further radial bubble growth this causes in turn causes further microlayer to be formed, which itself evaporates, and so on. The process of microlayer formation and evaporation is thus crucial to the understanding and modeling of bubble growth under a wide range of circumstances of practical importance.

Whilst the evaporation of such microlayers is incorporated to a degree in most modeling of bubble growth, it is based on essentially empirical representations of the dimensions of the microlayer. The actual hydrodynamic formation of these microlayers has been very little studied. In this paper we report investigations of formation of these microlayers via first-principles solution of the basic equations of fluid mechanics.

In Section 2 we summarise the experimental evidence for the existence of these microlayers, discuss qualitatively their (often dominant) effect on the growth of vapour bubbles, and summarise such earlier work as there is addressing their formation. In Section 3 we describe the modelling approach adopted for the microlayer formation simulations presented in this paper. In Section 4 we then present predictions of bubble growth and microlayer formation under various circumstances, making where we can comparisons with sophisticated modern experimental observations. In Section 5 we present further computations, attempting to develop and justify suggestions as to the underlying phenomena that govern the formation of the microlayer. Conclusions and suggestions as to where further work might be fruitfully conducted are presented in Section 6.

2 BACKGROUND

We will confine our discussion in this paper to water, although broadly similar observations would apply to other fluids (e.g. refrigerants), albeit naturally at different pressure and temperature combinations.

There is a wide range of pressure that is of industrial interest, ranging from, for example, the 150 bars within the primary circuit of a pressurised water reactor down to one bar (for example, following the same theme) under some fault conditions in a nuclear reactor.

There is similarly a wide range of wall superheats that are of practical interest. For obvious practical reasons the coverage with detailed experimental measurements of this parameter space is very uneven. There is coverage of a reasonable range of superheat at low pressure, but observations at higher pressures are very limited indeed. There are others, but we have attempted to show in Figure 1 the distribution of the main experimental observations upon which modellers typically rely for guidance and validation.

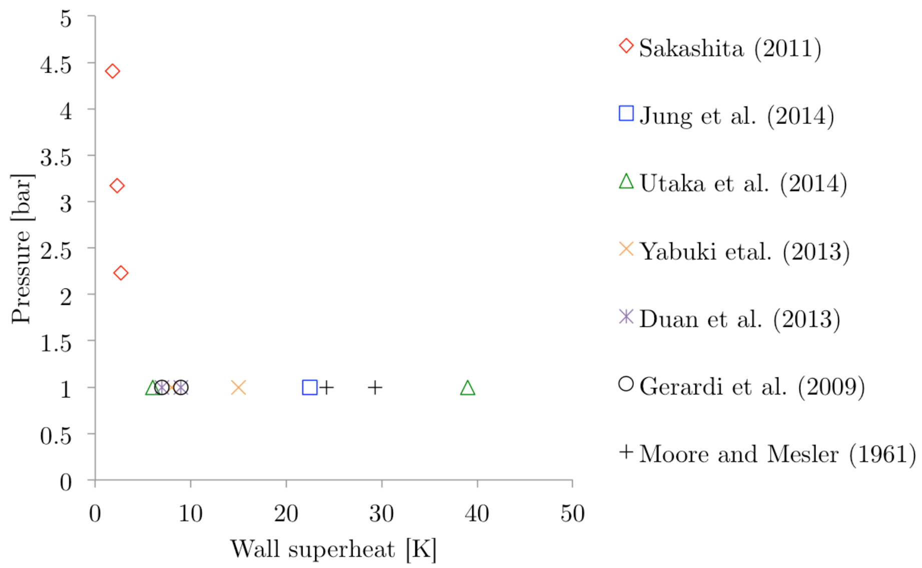

Figure 1
Overview of the main experimental data (Duan et al., 2013, Gerardi, 2009, Jung and Kim, 2014, Moore and Mesler, 1961, Sakashita, 2011, Utaka et al., 2014, Yabuki et al., 2013) available for nucleate boiling of saturated water.

2.1 Macroscopic bubble growth observations

The physical properties of water during boiling at (say) PWR-conditions are quite different from during boiling at atmospheric pressure. Surface tension is lower by a factor of 10, viscosity is lower by a factor of 4, and the vapour to liquid density ratio is lower by a factor of 2. As noted above, there are very few experimental studies under high-pressure conditions and the data available is limited to relatively low superheats of only a few Kelvin, and consequently slow bubble growth rates. The very tiny bubbles of ~100μm observed under these conditions remain spherical, and do not to trap microlayers at their underside (Sakashita, 2011).

In experimental studies of bubble growth at atmospheric pressure it is generally observed that at low growth rates bubbles remain more or less spherical, with no real microlayer being formed (Johnson et al., 1966). At higher growth rates the bubble shapes observed become more oblate and tend towards hemispherical. Typical departure diameters lie between 4 and 10mm. Experimental observations are that the flat underside of such oblate/hemispherical bubbles traps a thin layer of liquid, termed the 'microlayer', during the early stages of bubble growth (Jung and Kim, 2014, Utaka et al., 2014). Our study of microlayer formation thus will focus on low-pressure conditions.

A typical such bubble, photographed by Jung and Kim (2014), is shown in Figure 2. The 'apparent' contact angle is the tangent shown, based on macroscopic visual observation.

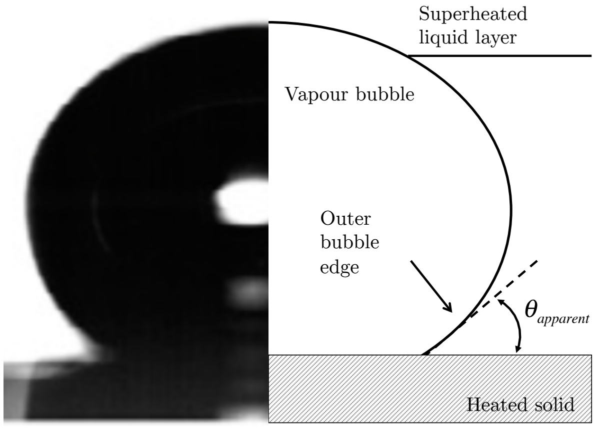

Figure 2
Macroscopic view of an oblate bubble growing at a heated wall at atmospheric pressure. Left: as measured by Jung and Kim (2014). Right: schematic diagram with apparent contact angle.

2.2 Microlayer experimental observations

There is by now convincing observational evidence for the existence of microlayers under atmospheric steam-water conditions. Snyder and Edwards (1956) were the first to hypothesize the existence of a thin liquid layer, which evaporates rapidly drawing substantial amounts of heat from the surface underneath a growing bubble. Later Moore and Mesler (1961) were able to provide qualitative verification of the existence of such microlayers by measuring temperature fluctuations on the surface underneath steam bubbles. In the following years other authors measured the thickness of this microlayer by interferometry, and by using temperature-time measurements of the surface [6-8].

More recent experimental investigations [9-12] have generated a consensus in the understanding of microlayers at atmospheric steam-water conditions. Their typical radial extent is about 1-2mm, with maximum thicknesses between 1-5μm [9-12]. Some typical measured microlayer dimensions are listed in Table 1.

	Wall superheat	Time to maximum microlayer radius	Maximum microlayer radius	Maximum microlayer thickness
	K	ms	mm	µm
Koffmann (1980)	n/a	n/a	0.25	1.85
Koffmann and Plesset (1983)	n/a	0.3	0.5	3
Kim and Buongiorno (2011)	n/k	1	1.5	5
Yabuki et al. (2013)	8	n/k	0.6	3
Yabuki et al. (2013)	16	n/k	0.9	5
Utaka et al. (2013)	20	n/k	0.388	1.5
Jung and Kim (2015)	22.5	1.67	1	3

Table 1
Measured initial microlayer characteristics for water boiling at atmospheric pressure.

In Figure 3 we show a diagram of the current consensus view of the microlayer configuration. The reason for the term 'apparent' contact angle is clear; there is not at this point a triple line, with liquid, vapour and solid all present. One does occur at a smaller radius, where the dry patch ends and the microlayer begins. Only after evaporation of the microlayer does the 'apparent contact angle' come to be associated with a triple line (Jung and Kim, 2014).

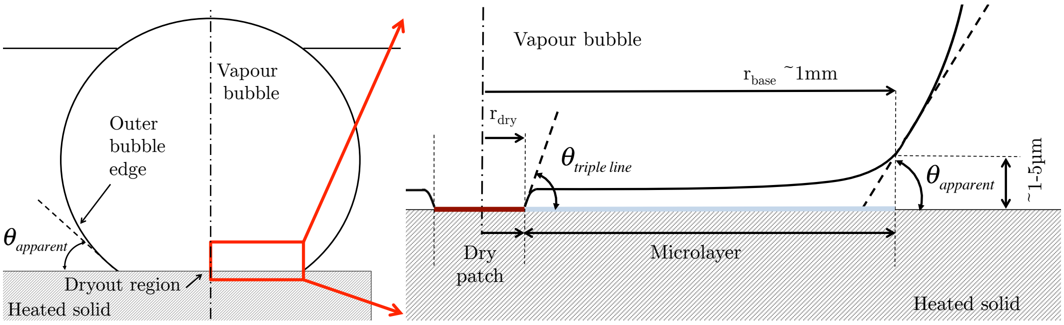

Figure 3
Detailed view of the underside of a bubble growing at a heated surface, representing the current consensus view. Not to scale / in proportion: Microlayer thicknesses are perhaps 1/50 to 1/500 of their radial extent.

2.3 Microlayers and bubble growth

As noted above, with their underside at the metal surface temperature, and their upper surface exposed to saturation temperature vapour, there is scope for a significant temperature difference through the microlayer, existing over a distance of only a few microns. The resulting heat flux and associated evaporation rate is thus large, and the microlayer thus is rapidly depleted.

There has been some discussion in the literature over the fraction of the total vapour entering the bubble that is generated from the microlayer.

To provide a simple estimate, we will take the fairly well characterised measurements of Jung and Kim (2015), as listed in Table 1 above. For the 2mm departure radius observed in this case, the 'conical wedge' shaped microlayer (taken to begin at a zero thickness at a zero radius) has a volume given by:

$$V_{ML} = \frac{2}{3}\pi r^2 \delta_{\max} \tag{1}$$

The ratio between the volume of steam from its evaporation, and the bubble volume at departure, is simply:

$$\frac{V_{ML_{VAPOUR}}}{V_{BUBBLE}} = \frac{\rho_l}{\rho_v}\frac{r_{MAX}^2}{r_{DEPARTURE}^2}\,\delta_{\max} \approx 0.62 \tag{2}$$

This suggests a possible contribution by the microlayer to vapour generation of order half.

With its small thickness, high heat fluxes through the microlayer are to be expected. Simplistically taking the temperature difference across it to be equal to the nominal wall superheat, again for the same Jung and Kim case (thickness say2 μm, superheat 10K), we would compute a heat flux of approximately

$$\dot{q}'' = \frac{k_l(T_W - T_{sat})}{\delta(r,t)} \approx 3\ \mathrm{MWm^{-2}} \tag{3}$$

Such high heat fluxes will however cause the local wall temperature to be reduced, and the reduction during the microlayer evaporation time will be a significant fraction of the superheat, requiring the inclusion of conjugate heat transfer in the analysis (Hänsch et al., 2015). There are also recent suggestions that for such heat fluxes the 'evaporative resistance' on the vapour side needs to be taken into account, as it could be comparable to, or even be greater than, the other resistances to heat transfer (Giustini et al., 2015).

Understanding and predicting bubble growth seems to depend heavily on understanding the behavior of the microlayer.

As the microlayer depletes it of course generates vapour rapidly, which causes further rapid bubble growth, which generally causes further microlayer to be left behind as the bubble expands, which in turn contributes further rapidly-generated vapour. This strong feedback mechanism makes the prediction of bubble growth and departure quite sensitive to the modeling of the microlayer.

2.4 The modeling of microlayers in bubble growth

The representation of microlayers in interface-tracking simulations aiming to model the growth and departure of single steam bubbles is troublesome. Since the microlayer formation and evaporation occurs at length scales ~two orders of magnitude smaller than the bubbles themselves, the mesh refinement required for resolving it directly is so stringent that first-principles modeling is not incorporated into microscopic CFD analysis of bubble growth. Instead, the process of microlayer evaporation is incorporated via semi-empirical 'sub-grid scale' models with approximate representation of the microlayer characteristics. The work of Sato and Ničeno (2015) was the first to incorporate such a 'sub-grid' model for microlayer evaporation into an interface-tracking code. The successful simulation of the growth and departure of single bubbles from a heated surface has been demonstrated.

In the CFD simulation itself, the vapour is taken to exist right up to the heated substrate. A microlayer thickness is associated with each CFD cell beneath the bubble adjacent to the heated wall. In each of these 'microlayer' cells a sub-grid calculation of the heat transfer through the microlayer is converted into an evaporation rate. This evaporation rate is used both to compute the reduction of the microlayer thickness until its depletion, and to apply a source of vapour at the heating surface that contributes to the growth of the bubble.

Parameters upon which the results of this sub-grid model depend are the initial microlayer thickness, and the variation of this thickness as the radial extent of the microlayer increases with the bubble growth. Parameters representing this have to be selected based on such limited quantified experimental evidence as is available for the case being studied. Provision of a sounder basis for the values to be used for this is indeed a major motivation for the present work.

As noted above, the sub-grid microlayer model needs also to evaluate conjugate heat conduction in the heated substrate, and the likely importance also of resistance to evaporative heat transfer has recently been demonstrated.

2.5 Microlayer hydrodynamic prediction

There has been published relatively little theoretical analysis of the formation of microlayers. There are several early works that attempt to explain the initial/isothermal (i.e. pre-evaporation) microlayer formation analytically. Based on the common understanding that the microlayer formation is determined by the flow of liquid within the microlayer, in 1969 (Cooper and Lloyd) and in 1975 (Van Stralen et al.) via different analyses arrived at similar expressions for the microlayer thickness as a function of time. Details are available in the two papers cited, but the resulting expressions were:

Cooper & Lloyd:

$$\delta_0 = \frac{\pi^2}{\pi^2+1}\frac{\sqrt{\pi}}{2}\sqrt{\upsilon_l t_g} \approx 0.8\sqrt{\upsilon_l t_g} \tag{4}$$

and Van Strahlen:

$$\delta_0 = 3.102(2\upsilon_l t_g)^{0.5}\,\mathrm{Pr}_l^{-0.33} \approx 3.632\sqrt{\upsilon_l t_g} \tag{5}$$

Here δ_0 is the predicted initial microlayer thickness at a certain location at the wall, t_g denotes the time it took the bubble to grow to that particular location. Pr_l and υ_l stands for the liquid Prandtl number and the liquid viscosity.

The resulting prediction of initial microlayer thickness is obtained as a function of radial position, and generally depends on the liquid viscosity and the growth time up to the particular radial location under consideration.

These models generally predict microlayer thicknesses grossly in excess of those observed in experiment. This is not surprising, as experimental observations of necessity are in circumstances where rapid microlayer depletion is taking place, and that process does not feature in either of these models.

Utaka and colleagues have more recently investigated the initial microlayer formation for elongated bubbles within micro-channels, and studied the effect of different physical conditions on the microlayer thickness (Utaka et al., 2009, Zhang et al., 2010, Zhang and Utaka, 2012, Zhang and Utaka, 2015). In micro-channels, it is suggested that microlayer thicknesses increase linearly with increasing viscosity and decreasing surface tension. Two different formation mechanisms were suggested; a low velocity surface tension and viscosity-controlled region, and a high velocity boundary layer-controlled region.

3 THE MODELLING APPROACH ADOPTED

3.1 Vapour generation

As noted above, we are at this stage addressing only the hydrodynamics of the formation of microlayers, with a (consciously non-physical) neglect of heat transfer and vapour generation. All of the results presented are isothermal.

We determine a source rate of vapour for the inflation of our bubble via a preliminary "off-line" calculation. This is done by specifying a time-dependent vapour evolution rate that is taken to obtain over the curved liquid-vapour interface. It is important to ensure to be sure that physically realistic rates, and in particular physically realistic temporal dependence of this rate, are employed. To achieve this we used the solution of Scriven (1959) at various superheats to determine the time dependence of the vapour mass flux. There is thus no direct and mechanistic connection between the superheat applied in this Scriven calculation, and the superheat of the heating surface for which we are modeling the growth of a bubble, since the thermal conditions are not identical. However, since the growth of a bubble at a heated wall is actually really rather similar to and surprisingly well approximated by a Scriven solution, we can make a reasonable association between the experimental superheat of the case studied and the notional superheat used in our computation of vapour evolution rate.

We employed four different growth rates, listed in Table 2.

To avoid depleting the microlayer itself, the vapour evolution used in the model, at the vapour mass flux computed as outlined above, was applied only to that bubble surface a height of 10 μm or more above the heated substrate.

Parameters	Rate 1	Rate 2	Rate 3	Rate 4
Scriven ΔT [K]	5	10	15	18.5
Ja number	15.4	30.9	46.4	57.2
Rtrans [μm]	25	72	132	180
Simulation specifications				
Seed size [μm]	30	80	140	185
Initial time [μs]	5.94	10.8	14.85	17.08
Initial mdot [kg/m^2s]	1.46	2.14	2.73	3.13

Table 2
Parameters used in the simulations at each of the four growth rates considered.

For the three 'Scriven ΔT' values used, the computed solution for bubble radius versus time is shown in Figure 4.

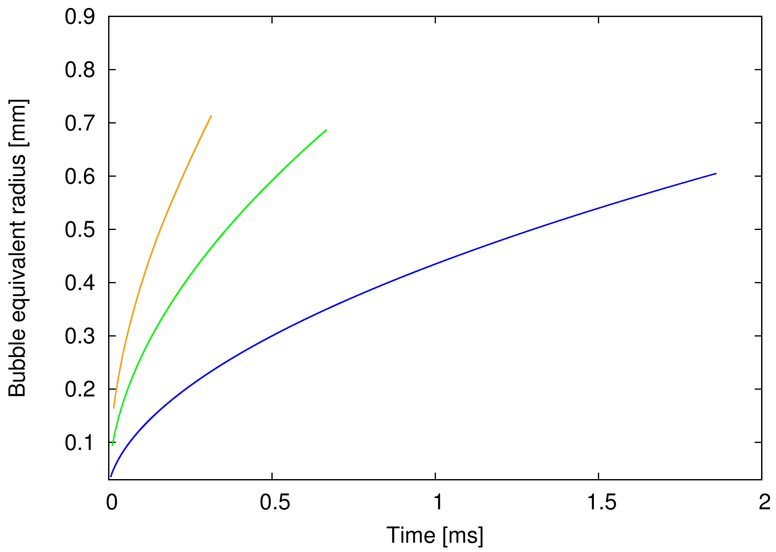

Figure 4
Computed bubble growth rates using the Scriven solution for the different superheats. Blue: 5K, Green: 10K and Yellow: 15 K.

A further 'Scriven superheat', of 18.5K, was selected by trial and error to give an equivalent temporal dependence of bubble radius to that measured in one of the experimental measurement cases we use for comparison. This is shown in Figure 5.

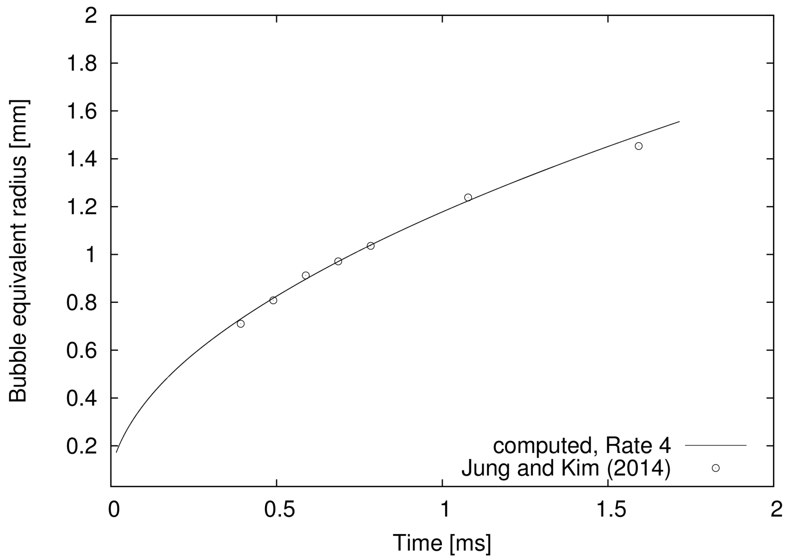

Figure 5
Computed bubble growth rate using the Scriven solution for a superheat of ΔT=18.5K, compared to the measurements of Jung and Kim (2014).

3.2 Computational issues

For the computational studies presented in this paper an axis-symmetric domain was used, as illustrated in Figure 6. The focus of the computations is on the region in close proximity to the wall and the mesh was refined considerably there.

A grid convergence study was performed for the vapour generation with Rate 2. Following this study a computational domain of 350x350 cells, with the finest mesh size 1μm, was adopted for the rest of the computations. Whilst an even finer resolution of the liquid layer would be desirable, a major practical problem in the simulations is the tiny time steps required. Typically, time steps of about 10 nanoseconds were required to meet Courant limits of ~0.3, which coupled to the 2 millisecond duration of bubble growth that is simulated results in inconveniently long runtimes.

For the last case with Rate 4 the computational domain had to be increased in extent in order to allow the investigation of the very fast growing bubble. A domain of 3x3mm was used with 400x400cells, with the finest mesh size near the wall of ~2μm.

For the computations the interface-tracking code TransAT (ASCOMP, 2015) was used. This is a sophisticated research-level finite-volume code that is widely used for fundamental two-phase flow studies (Lakehal et al., 2002, Narayanan and Lakehal, 2008). The gas-liquid interface is tracked using the level-set method, where the interface evolves via a scalar distance function. Possible deformations of the level-set field due to numerical errors were prevented by using a third-order WENO re-distancing algorithm (Sussmann et al., 1994).

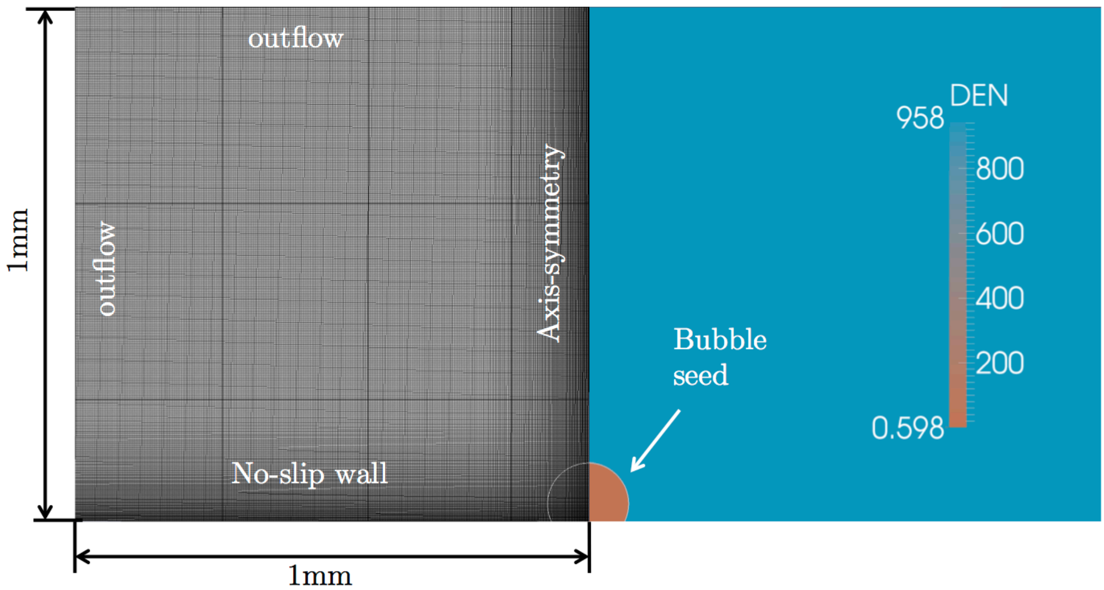

Figure 6
Computational domain with applied boundary conditions (left) and the initial conditions for Rate 2 (right).

3.3 Liquid – solid contact angle

Recall that the normal "apparent" contact angle does not require to be specified in our computations. Indeed, it is automatically computed, in that the shape of the interface throughout that region is part of the solution. The only place where it is necessary to impose some model of the interaction between the vapour, liquid and solid is at the inboard end of the microlayer.

This is not a quantity that it is practicable to measure, and any value we insert must necessarily be somewhat arbitrary. Lacking justification for anything different, in effect we imposed a contact angle of 90°. That is, we imposed a form of contact angle where the interface condition itself presented no resistance to the motion of the interface.

4 PREDICTIONS OF MICROLAYER BEHAVIOUR

4.1 Bubble evolution and microlayer extent.

We show in Figure 7 the evolution of the bubble size and shape for each of the first three growth rates.

For the slow growth, Rate 1, we see a generally spherical bubble, with small if any microlayer being formed. For Rate 2 the bubble is distinctly non-spherical or oblate, and there is plainly a quite extensive microlayer that grows as the bubble expands. This is considerably more marked in the Rate 3 case, where the overall shape is tending towards hemispherical.

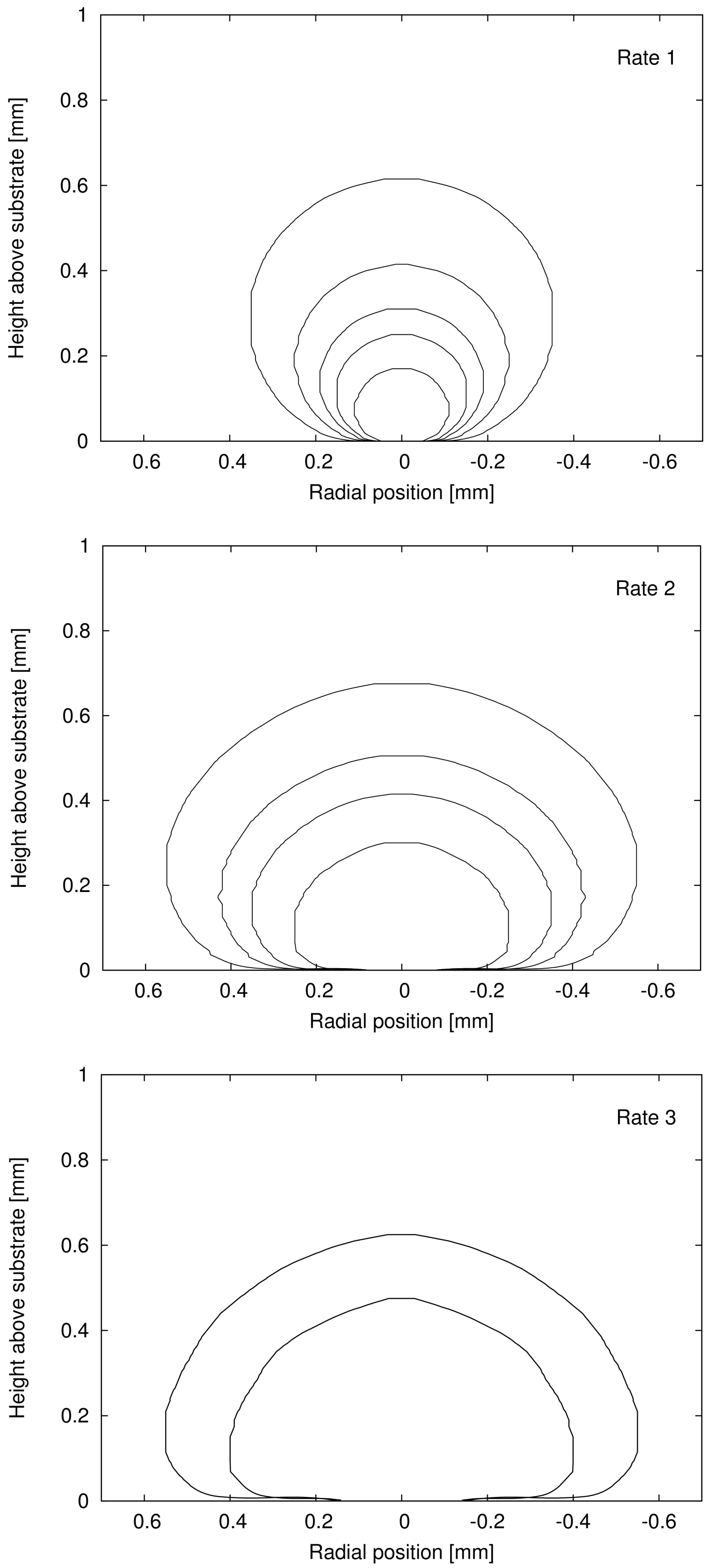

Figure 7
Computed bubble outlines at a series of times for Rates 1, 2 and 3, at times:
Rate 1: 0.1, 0.2, 0.3, 0.5, 1.0ms, Rate 2: 0.1, 0.2, 0.3, 0.5ms, Rate 3: 0.1, 0.2ms.

In Figure 8 results for all three rates are shown when the bubbles have reached an equivalent bubble radius of 0.6mm, after times of 1.84, 0.5 and 0.23ms for the different growth rates respectively. The progression to a shorter, wider bubble, with a more extensive microlayer, is clear.

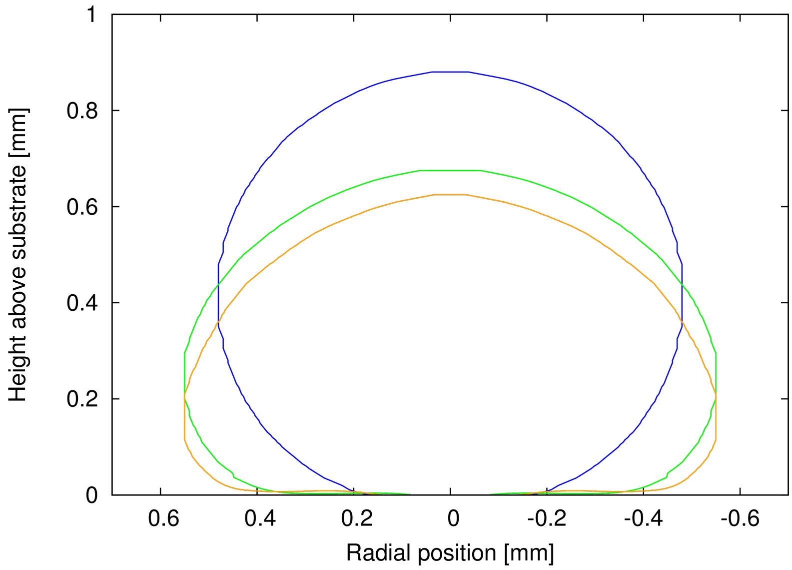

Figure 8
Comparison of bubble shapes for the three growth rates, at the same bubble equivalent radius of 0.6mm, after 1.84ms for Rate 1 (Blue), 0.5ms for Rate 2 (Green) and 0.23ms for Rate 3 (Yellow) respectively.

In Figure 9 we show a comparison of the bubble shapes for the '18.5K Scriven' superheat, selected to give a vapour evolution rate that broadly matches that of the Jung and Kim measured case. There are evidently some gaps in the measured data, but the simulations are in excellent qualitative, and fairly good quantitative agreement with the observations.

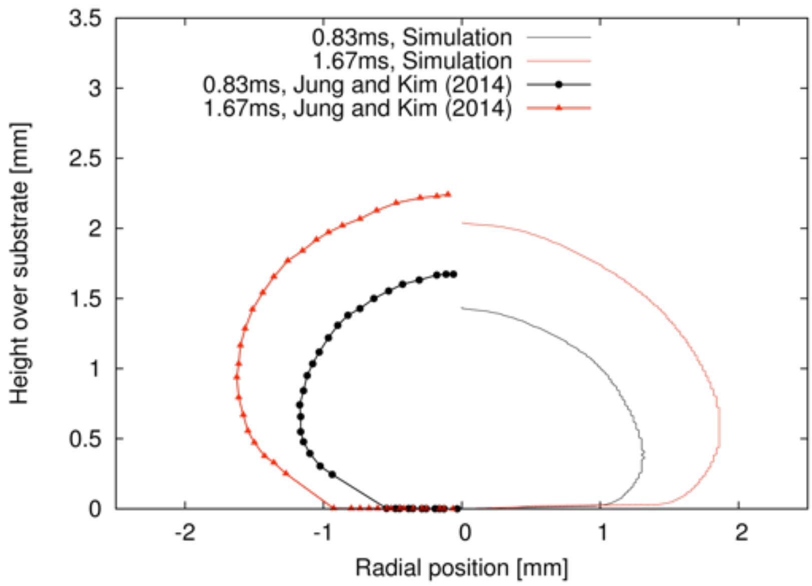

Figure 9
Bubble shapes after 0.83ms and 1.67ms compared to the experimental observations of Jung and Kim (2014).

It is helpful to see the macroscopic flow fields responsible for these bubble growths. For Rate 2, at times of 0.1, 0.2 and 0.3ms we show vector and streamline plots of the flow field in Figure 10. Of these, it is the flows in the liquid, caused as they are by the growth of the vapour bubble, that are of greatest importance. In general this flow is more or less purely radially outwards, but near the wall the speed is much reduced by the non-slip condition, and some liquid is 'left behind', with the vapour riding up over it, forming the microlayer.

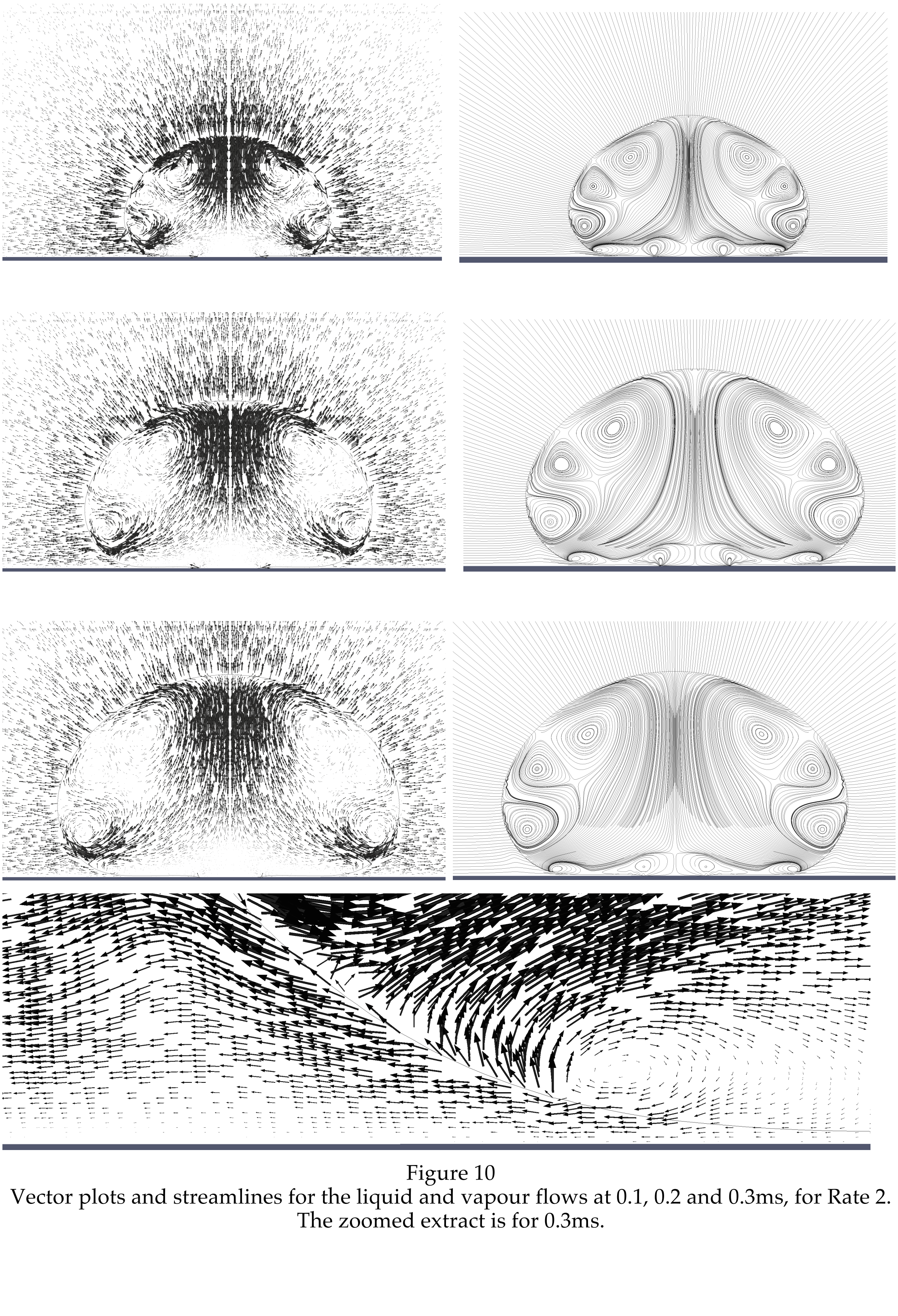

Figure 10
Vector plots and streamlines for the liquid and vapour flows at 0.1, 0.2 and 0.3ms, for Rate 2.
The zoomed extract is for 0.3ms.

4.2 Microlayer evolution

In Figure 11 we show the evolution of the microlayer in more detail than is visible in the 'whole bubble' views of Figure 7. The near-absence of a microlayer at the low growth rate, and the liquid layer's increase in both radial extent and thickness with growth rate, is clear. This is confirmed in Figure 12, where at a given bubble size the microlayer radial extent and thickness are both seen to increase with growth rate.

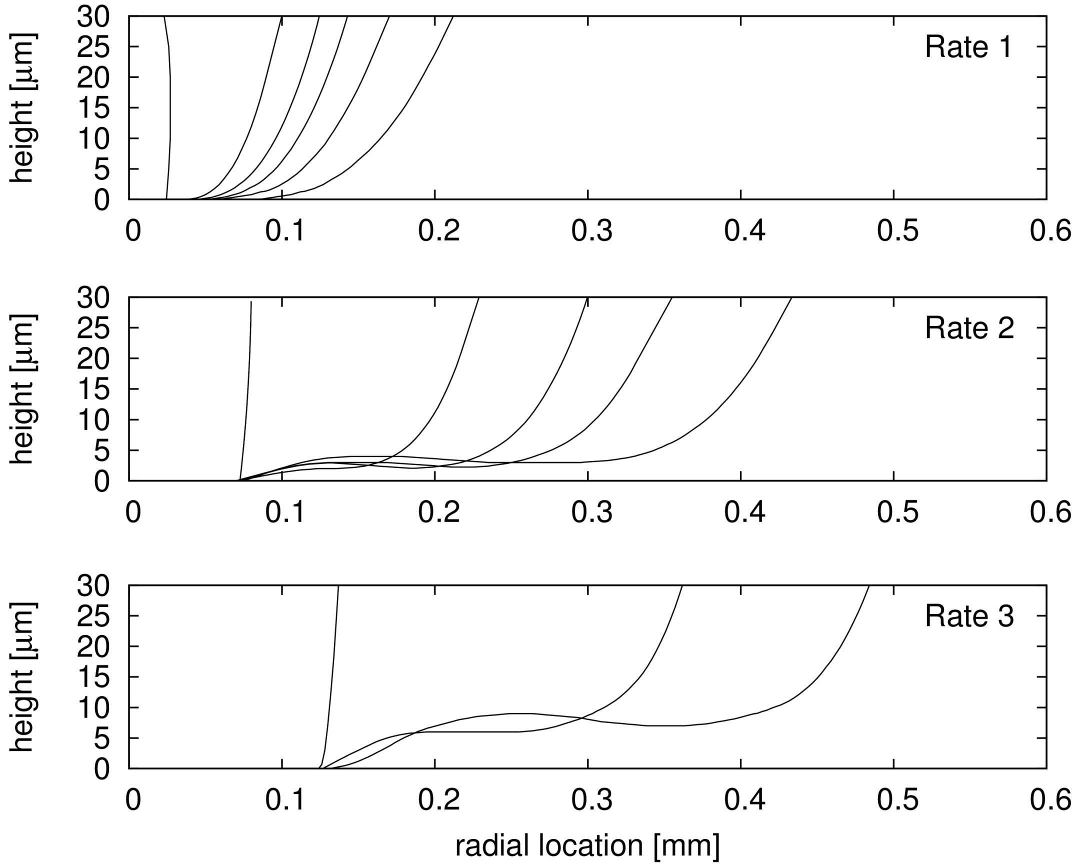

Figure 11
Interface outlines for Rates 1 2 & 3: Rate 1: 0.0, 0.1, 0.2, 0.3, 0.5 and 1.0ms, Rate 2: 0.0, 0.1, 0.2, 0.3, 0.5ms, Rate 3: 0.0, 0.1, 0.2ms.

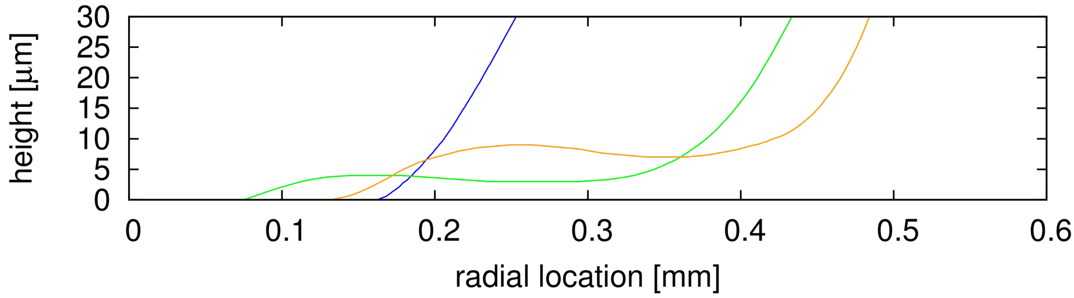

Figure 12
Interface outlines for Rates 1, 2 and 3 at the same bubble equivalent diameter. Blue: Rate 1 at 1.84ms, Green: Rate 2 at 0.5ms, Yellow: Rate 3 at 0.23ms.

As discussed earlier, we are here focusing our attention on the hydrodynamics of the formation of the microlayer, and are not modeling at all its depletion. Accordingly, we cannot usefully make comparisons of the present predictions of microlayer thickness with experimental observations.

We can to a degree compare with the earlier analytical suggestions, and we do this in Figure 13. The present computations lie between the two proposed analytical models.

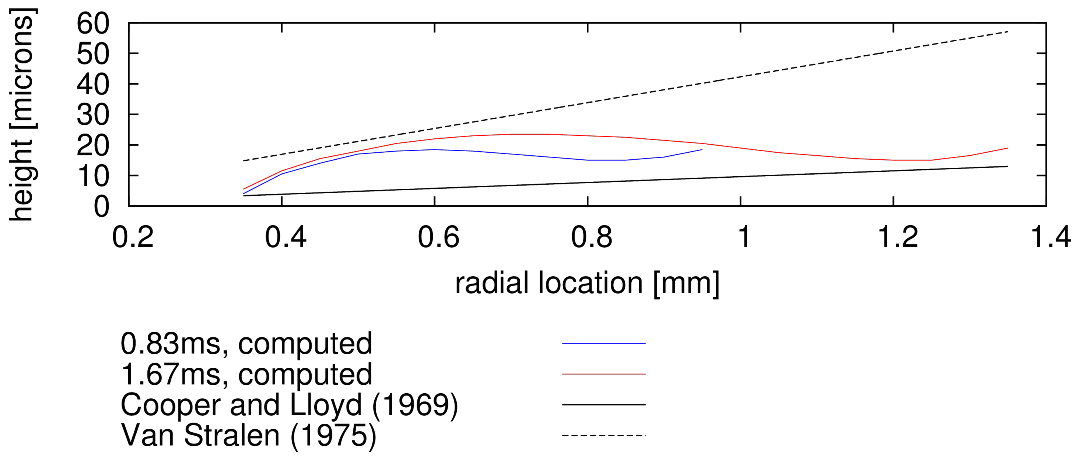

Figure 13
The microlayer profiles for the fourth "18.5 K" rate, evaluated at 0.83 and 1.67ms, compared with the analytical forms proposed by each of Cooper and Lloyd (1969) and Van Stralen et al. (1975).

4.3 Velocity profiles within the microlayer over time

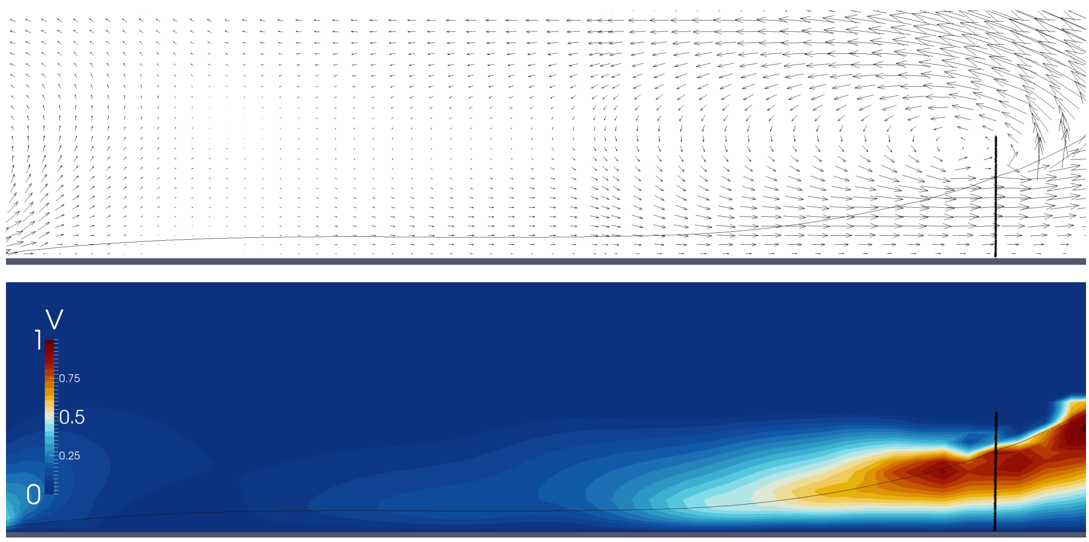

Figure 14
Detailed view of the underside of the bubble (with a radial extent ranging from 80 to 210μm and a height of 30μm).
Top: Velocity vectors in close proximity to the wall for Rate 2 after 0.1ms (This is early in the overall process; to give a sense of scale, the time to departure would be ~100 times longer).
Bottom: The corresponding velocity field.
The dark line at a radial position of 200μm indicates the location for the velocity plot in Figure 15.

We show in Figure 14 the velocity distribution in the microlayer, for Rate 2, after 0.1ms. The near absence of flow in the inboard, 'level topped, formed' microlayer is clear, as is the effect of the no-slip wall in inhibiting the radially outward flow of the liquid as the interface advances. At a radial location of 0.2mm we show in Figure 15 the radial component of velocity, at this 0.1ms time, and at three later times. The sharp reduction in flow in the liquid once the microlayer has formed is clear.

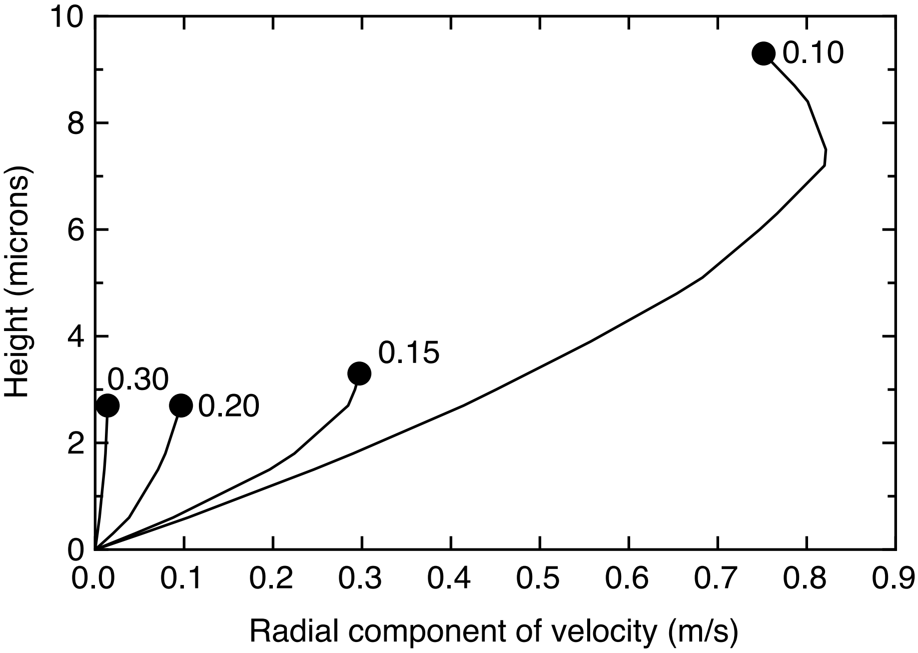

Figure 15
Velocity profiles at a radial position of 200μm for Rate 2, at the times (in milliseconds) indicated. The black circles indicate the liquid thickness at each time.

5 MICROLAYER FORMATION

5.1 The determinants of the formation or otherwise of a microlayer, and of its extent

The results presented thus far indicate clearly that low growth rates are associated with no microlayer formation, and higher growth rates tend to cause a microlayer to be formed. This is associated with the degree to which the growing bubble retains a broadly spherical shape, or tends to become more hemispherical.

The tendency to retain its spherical shape or otherwise is a result of the competition between the surface tension, which is tending to cause the bubble to be a sphere, and the need for the growing bubble to overcome the inertia of the fluid above it that needs to be displaced to accommodate it. This tends to flatten the bubble.

It is straightforward to confirm both of these inferences by numerical experiment.

In Figure 16 we see the role played by surface tension in determining bubble shape. Reduction is seen to allow the bubble to be forced to a more oblate shape, with the extent of the ~flat base in near-contact with the solid surface increased.

In Figure 17 we see the effect of making the bubble's growth away from the wall easier or more difficult, by decreasing and increasing the density of the fluid it must displace. A strong dependence on density is exhibited, explaining the rate-dependence in terms of the inertial restraints the growing bubble needs to overcome.

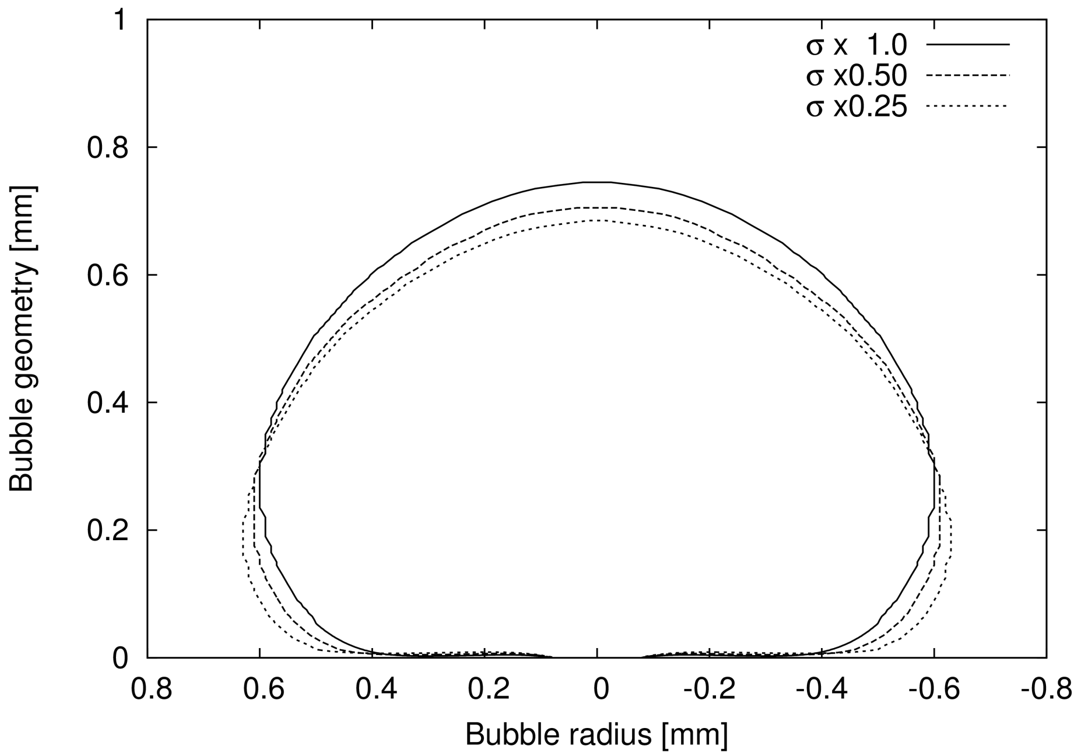

Figure 16
The influence of reduced surface tension on the bubble shape (Growth Rate 2, 0.6ms).

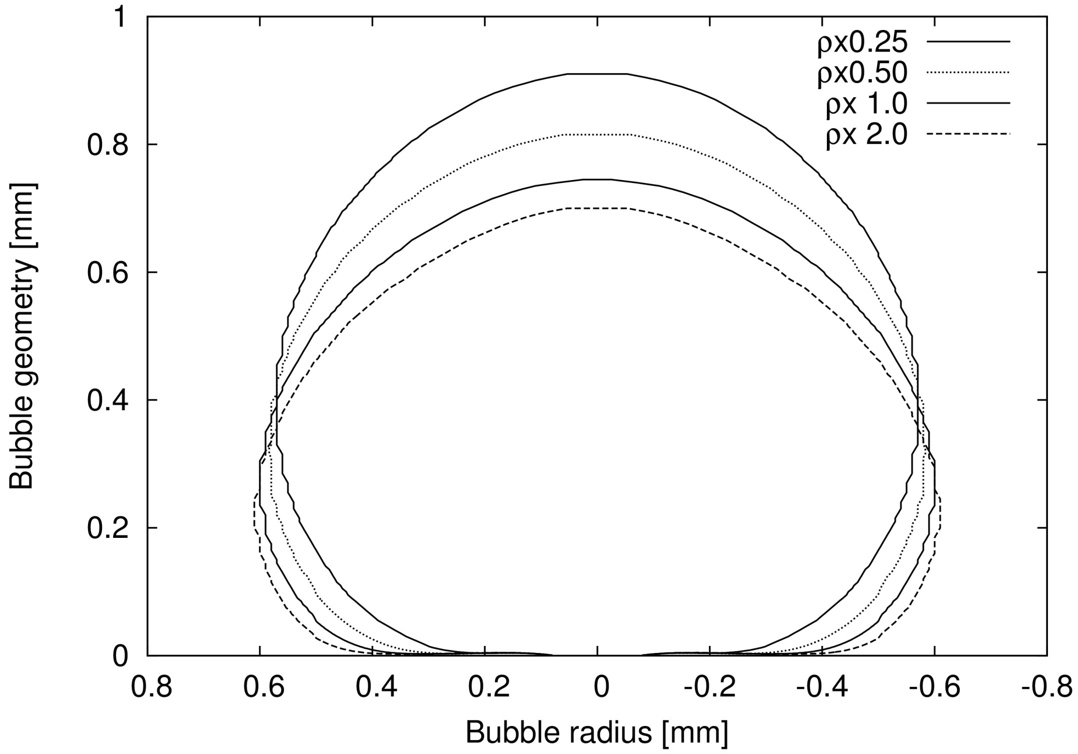

Figure 17
The influence of density on the bubble shape (Growth rate 2, 0.6ms).

5.2 The microlayer thickness

5.2.1 Density

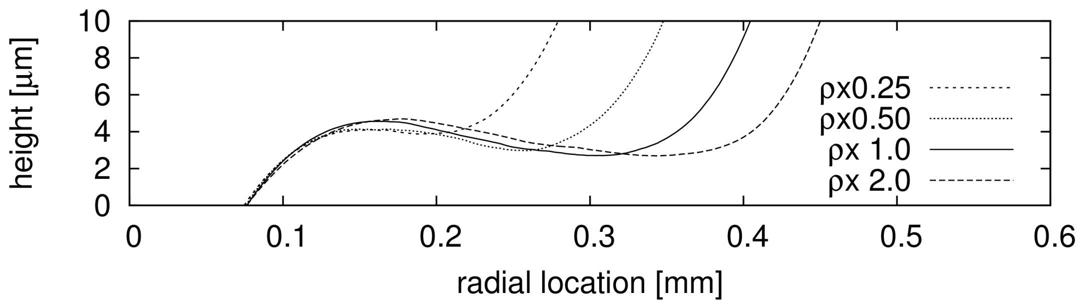

Figure 18
The effect of density on the microlayer thickness and extent (Growth rate 2, 0.6ms).

Figure 18 is a much-zoomed extract of Figure 17 (and note that whereas the vertical and horizontal scales in the latter are equal, in the extract the vertical scale is greatly increased). We see here the effect of the varying density, and associated slower growth rate as density increases, on the microlayer thickness and extent. This is broadly consistent with the dependence on growth rate already observed in Figure 11, where generally similar shapes, but larger radial extents, accompany higher growth rates.

5.2.2 Surface tension

In Figure 19, a similarly zoomed-in version of Figure 16, we see the effect on the microlayer of the reduced surface tension. In causing the bubble to become more oblate, the surface tension causes the microlayer thickness and radial extent to increase.

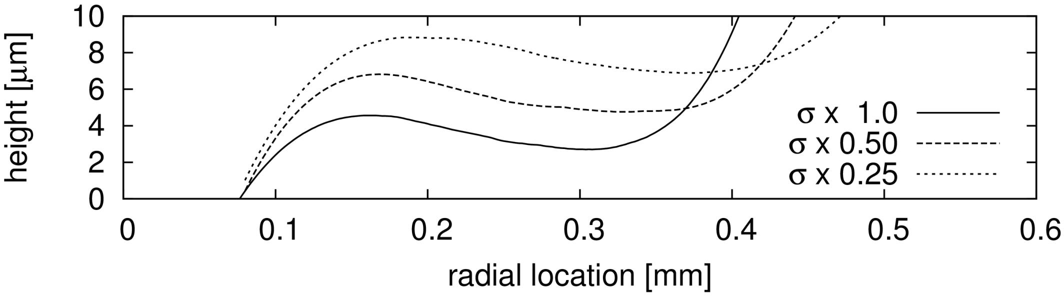

Figure 19
The effect of surface tension on the microlayer thickness and extent (Growth rate 2, 0.6ms).

5.2.3 Viscosity

Viscosity has modest effect on the overall bubble shape, and hence microlayer extent, an increase in viscosity has, as would be expected, the effect of increasing the microlayer thickness. This is seen in Figure 20.

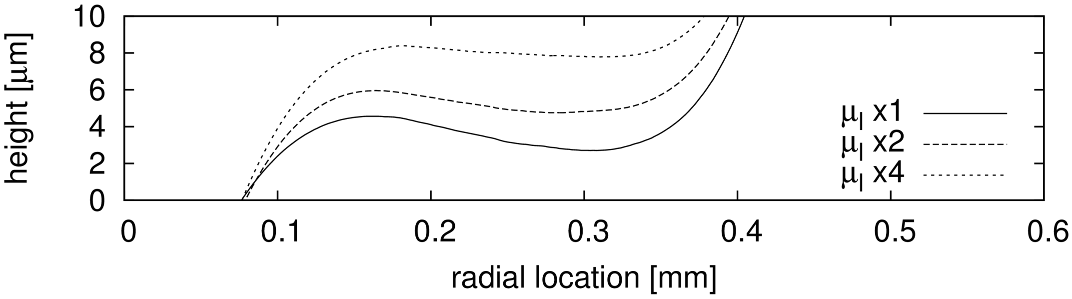

Figure 20
The effect of viscosity on the microlayer thickness and extent (Growth rate 2, 0.6ms).

6 CONCLUSIONS

It is clear from multiple experimental observations that under certain conditions bubbles that nucleate and grow in the vicinity of a heated wall do so leaving beneath them a very thin film of liquid water as the area of their base in "contact" with the heated wall expands radially. Being so thin, this film evaporates very rapidly, and can contribute possibly the majority of the vapour required to cause the bubble to be of a size to depart from the wall.

The importance of this microlayer is particularly acute because as it evaporates, generating vapour rapidly, it is itself the cause of further rapid bubble growth, which causes additional microlayer to be generated, which then in turn evaporates, and so on. There is thus a strong feedback mechanism, making a good understanding of the formation of the microlayer particularly important.

Presently representation of this microlayer is included in microscopic boiling analyses in a relatively simple fashion, with its geometry characterised necessarily rather crudely, based upon the very limited amount of quantitative experimental evidence that is available.

As the beginning of an attempt to address this, we have here presented mechanistic first-principles calculations of the hydrodynamics of the formation of the microlayer. This has allowed what we believe to be the underlying physical mechanisms behind its formation to be identified with reasonable confidence.

In essence, we conclude that the principal determinant of the existence and radial extent of the microlayer is the bubble growth rate, with a high growth rate, and the associated inertial effects, counteracting the influence of the surface tension in maintaining sphericity of the bubble.

All of this present work has been performed addressing solely the hydrodynamics of the formation of the microlayer. A comprehensive model will require that the depletion of the microlayer through its rapid evaporation should also be included, and this is a natural area for further work.

7 ACKNOWLEDGEMENTS

The financial support by the ASCOMP GmbH for one of us (SH) is gratefully acknowledged. It is a pleasure to acknowledge helpful discussions with Chidambaram Narayanan of ASCOMP regarding the TransAT code, and with Hyungdai Kim, of Kyung Hee University, Seoul, regarding their experimental measurements.

8 REFERENCES

ASCOMP 2015. TransAT Handbook Series. Multiphase Flow Modelling.

COOPER, M. G. & LLOYD, A. J. P. 1969. The microlayer in nucleate pool boiling. *International Journal of Heat and Mass Transfer,* 12**,** 895-913.

DUAN, X., PHILLIPS, B. & BUONGIORNO, J. 2013. Synchronized High-Speed Video, Infrared Thermometry, and Particle Image Velocimetry Data for Validation of Interface-Tracking Simulations of Nucleate Boiling Phenomena. *Experimental Heat Transfer,* 26**,** 169-197.

GERARDI, C. D. 2009. *Investigation of the Pool Boiling Heat Transfer Enhancement of Nano-Engineered Fluids by means of High-Speed Infrared Thermography.* PhD, Massachusetts Institute of Technology.

GIUSTINI, G., JUNG, S., KIM, H. & WALKER, S. P. 2015. Evaporative thermal resistance and its influence on microscopic bubble growth. *International Journal of Heat and Mass Transfer (In press).*

HÄNSCH, S., NARAYANAN, C., REBOUX, S., GIUSTINI, G. & WALKER, S. 2015. Microlayer Models for Nucleate Boiling Simulations: The Significance of Conjugate Heat Transfer. *Nureth-16.* Chicago, USA.

JOHNSON, M. A., JAVIER DE LA PEÑA, J. & MESLER, R. B. 1966. Bubble Shapes in Nucleate Boiling. *AIChE Journal,* 12**,** 344-348.

JUNG, S. & KIM, H. 2014. An experimental method to simultaneously measure the dynamics and heat transfer associated with a single bubble during nucleate boiling on a horizontal surface. *International Journal of Heat and Mass Transfer,* 73**,** 365-375.

JUNG, S. & KIM, H. 2015. An Experimental Study on Heat Transfer Mechanisms in the Microlayer using Integrated Total Reflection, Laser Interferometry and Infrared Thermometry Technique. *Heat Transfer Engineering,* 36**,** 1002-1012.

KIM, H. & BUONGIORNO, J. 2011. Detection of liquid–vapor–solid triple contact line in two-phase heat transfer phenomena using high-speed infrared thermometry. *International Journal of Multiphase Flow,* 37**,** 166-172.

KOFFMANN, L. D. 1980. *I. Experimental observations of the microlayer in vapor bubble growth on a heated solid. II. An investigation of the theory of evaporation and condensation.* . PhD, California Institute of Technology.

KOFFMANN, L. D. & PLESSET, M. S. 1983. Experimental Observations of the Microlayer in Vapor Bubble Growth on a Heated Solid. *Journal of Heat Transfer,* 105**,** 625-632.

LAKEHAL, D., MEIER, M. & FULGOSI, M. 2002. Interface tracking towards the direct simulation of heat and mass transfer in multiphase flows. *International Journal of Heat and Fluid Flow,* 23**,** 242-257.

MOORE, F. D. & MESLER, R. B. 1961. The Measurement of Rapid Surface Temperature Fluctuations During Nucleate Boiling of Water. *AIChE Journal,* 7**,** 620-624.

NARAYANAN, C. & LAKEHAL, D. 2008. Two-Phase Convective Heat Transfer in Miniature Pipes Under Normal and Microgravity Conditions. *Journal of Heat Transfer,* 130.

SAKASHITA, H. 2011. Bubble Growth Rates and Nucleation Site Densities in Saturated Pool Boiling of Water at High Pressures. *Journal of Nuclear Science and Technology,* 48**,** 734-743.

SATO, Y. & NIČENO, B. 2015. A depletable micro-layer model for nucleate pool boiling. *Journal of Computational Physics,* 300**,** 20-52.

SCRIVEN, L. E. 1959. On the dynamics of phase growth. *Chemical Engineering Science,* 10**,** 1-13.

SNYDER, N. R. & EDWARDS, D. K. Summary of Conference on Bubble Dynamics and Boiling Heat Transfer. 14-15 June 1956 Jet Propulsion Laboratory.

SUSSMANN, M., SMEREKA, P. & OSHER, S. 1994. A level set approach for computing solutions to incompressible two-phase flow. *Journal of Computational Physics,* 114**,** 146-159.

UTAKA, Y., KASHIWABARA, Y. & OZAKI, M. 2013. Microlayer structure in nucleate boiling of water and ethanol at atmospheric pressure. *International Journal of Heat and Mass Transfer,* 57**,** 222-230.

UTAKA, Y., KASHIWABARA, Y., OZAKI, M. & CHEN, Z. 2014. Heat transfer characteristics based on microlayer structure in nucleate pool boiling for water and ethanol. *International Journal of Heat and Mass Transfer,* 68**,** 479-488.

UTAKA, Y., OKUDA, S. & TASAKI, Y. 2009. Configuration of the micro-layer and characteristics of heat transfer in a narrow gap mini/micro-channel boiling system. *International Journal of Heat and Mass Transfer,* 52**,** 2205-2214.

VAN STRALEN, S. J. D., SOHAL, M. S., COLE, R. & SLUYTER, W. M. 1975. Bubble growth rates in pure and binary systems: Combined effect of relaxation and evaporation microlayers. *International Journal of Heat and Mass Transfer,* 18**,** 453-467.

YABUKI, T., SAITOH, T. & NAKABEPPU, O. 2013. Contribution of microlayer evaporation to bubble growth in pool saturated boiling of water. *ASME 2013 11th International Conference on Nanochannels, Microchannels, and Minichannels.* Sapporo, Japan.

ZHANG, Y. & UTAKA, Y. 2012. Characteristics of Microlayer Formation and Heat Transfer in Mini/Microchannel boiling systems : A Review *Frontiers in Heat and Mass Transfer,* 3.

ZHANG, Y. & UTAKA, Y. 2015. Characteristics of a liquid microlayer formed by a confined vapor bubble in micro gap boiling between two parallel plates. *International Journal of Heat and Mass Transfer,* 84**,** 475-485.

ZHANG, Y., UTAKA, Y. & KASHIWABARA, Y. 2010. Formation Mechanism and Characteristics of a Liquid Microlayer in Microchannel Boiling System. *Journal of Heat Transfer,* 132.